



Reducing Data Uncertainty in Forest Fire Spread Prediction: A Matter of Error Function Assessment

Carlos Carrillo^(✉), Ana Cortés, Tomàs Margalef, Antonio Espinosa,
and Andrés Cencerrado

Computer Architecture and Operating Systems Department,
Universitat Autònoma de Barcelona, Barcelona, Spain
{carles.carrillo, ana.cortes, tomas.margalef, antoniomiguel.espinosa,
andres.cencerrado}@uab.cat

Abstract. Forest fires are a significant problem that every year causes important damages around the world. In order to efficiently tackle these hazards, one can rely on forest fire spread simulators. Any forest fire evolution model requires several input data parameters to describe the scenario where the fire spread is taking place, however, this data is usually subjected to high levels of uncertainty. To reduce the impact of the input-data uncertainty, different strategies have been developed during the last years. One of these strategies consists of adjusting the input parameters according to the observed evolution of the fire. This strategy emphasizes how critical is the fact of counting on reliable and solid metrics to assess the error of the computational forecasts. The aim of this work is to assess eight different error functions applied to forest fires spread simulation in order to understand their respective advantages and drawbacks, as well as to determine in which cases they are beneficial or not.

Keywords: Error function · Wild fire · Prediction · Data uncertainty

1 Introduction

As it is known, forest fires are one of the most destructive natural hazards in the Mediterranean countries because of their significant impact on the natural environment, human beings and economy. For that reason, scientific community has invested lots of efforts in developing forest fire propagation models and computational tools that could help firefighter and civil protection to tackle those phenomena in a smart way in terms of resources allocation, extinguish actions and security. The quality results of these models depend not only on the propagation equations describing the behaviour of the fire, but also on the input data required to initialize the model. Typically, this data is subjected to a high

degree of uncertainty and variability during the evolution of the event due to the dynamic nature of some of them such as meteorological conditions or moisture contents in the vegetation. Any strategy oriented to reduce this input data uncertainty requires a quality measure of the results to determine the goodness of the proposed strategy. Typically, on the forest fire spread prediction field, this assessment relies on a fitness/error function that must evaluate how well the prediction system reproduces the real behaviour of the fire. In order to speed up the process of finding good estimations of certain input parameters, the prediction systems tend to include a calibration stage prior to perform the forest fire spread prediction (prediction stage) [4]. In particular, we focus on a well know two-stage methodology, which is based on Genetic Algorithms (GA). In this scheme, the calibration stage runs a GA to reduce input data uncertainty. To do that, the GA generates an initial population (set of individuals) where each individual consists of a particular configuration of the input parameters from which reducing their uncertainty implies an improvement in terms of quality results. This initial population will evolve using the so called genetic operators (elitism, mutation, selection, crossover) to obtain an improved set of individuals that better reproduces the observed past behaviour of the fire. After several iterations of the GA, the best individual will be selected to predict the near future (prediction stage). A key point in all this process is the error function applied to determine the prediction quality of each individual. This function drives the GA's evolution process, consequently, to establish an appropriate level of confidence in the way that the error function is assessed is crucial in the system, [2].

The goal of this work is to study and test eight different error functions to assess the simulation error in the case of forest fire spread prediction.

This paper is organized as follows. In Sect. 2 the data uncertainty problem when dealing with forest fires spread prediction and how it can be minimize with an appropriate error function selection is introduced. Section 3 details an analysis of the different proposed functions to compute the simulation error. Section 4 presents the experimental results and, finally, Sect. 5 summarizes the main conclusions and future work.

2 Reducing Input Data Uncertainty

In order to minimize the uncertainty in the input data when dealing with forest fire spread prediction, we focus on the Two-Stage prediction scheme [1]. The main goal of this approach is to introduce an adjustment stage previous to the prediction stage to better estimate certain input parameters according to the observed behaviour of the forest fire. The main idea behind this strategy is to extract relevant information from the recent past evolution of the fire that could be used to reduce data uncertainty in the near future forecast. As it has previously mentioned, this scheme relies on a GA. Each individual of the GA population consists of a particular input parameter setting that will be fed into the underlying forest fire spread simulator. In this work, the forest fire spread simulator used is FARSITE [7], however, the methodology described would be

reproduced for any other simulator. Each simulation generates a forest fire propagation that must be compared to the real evolution of the fire. According to the similarity in terms of shape and area among the simulated propagation and the real fire behaviour, the corresponding input parameters set is scored with an error value. Typically, low errors indicates that the provided forecast is closer to the reality, meanwhile higher errors indicate certain degree of mismatching between the two propagations.

There are several metrics to compare real and simulated values and each one weighs the events involved differently, depending on the nature of the problem [2]. In the forest fire spread case, the map of the area where the fire is taking place is represented as a grid of cells. Each cell is labeled to know if it has been burnt or not in both cases: the real propagation map and the simulated fire spread map. Then, if one compare both maps cell by cell, we came up with different possibilities: cells that were burnt in both the actual and simulated spread (*Hits*), cells burnt in the simulated spread but not in the reality (*False Alarms*), cells burnt in the reality but not in the simulated fire (*Misses*) and cells that were not burnt in any case (*Correct negatives*) [6, 8]. These four possibilities are used to construct a 2×2 contingency table, as is shown in Fig. 1.

		Observation	
		Yes	No
Prediction	Yes	HITS	FALSE ALARM
	No	MISSES	CORRECT NEGATIVES

Fig. 1. Standard structure of a contingency table.

Nevertheless, at the time to put a prediction system into practice, it is important to consider what a *good forecast* actually means, according to the underlying phenomena we are dealing with, since there are many factors that models do not take into account. In our case, when a fire is simulated, a free fire behavior is considered, without including human intervention (firefighters). Under this hypothesis, the simulations should overestimate the burnt area. For this reason, when a simulation produces an underestimated perimeter (front of the fire), it is considered a bad result. Because of this, we are interested in those error functions that minimize the impact of *False Alarms* above the impact of *Misses*. Let's imagine two hypothetical forest fire spread predictions where the number of FA in one of them is the same value that the number of Misses in the other one. Under this assumption, we would expect that the error function provides a lower error in the first case than in the second case.

In addition, for the particular case of forest fire spread forecast, the cells labeled as correct negatives are ignored because the area of the map to be

simulated may vary independently of the fire perimeter, so they may distort the measurement of the error. In the following section, a description of the different error functions analyzed in this work is done.

3 Error Function Description

We propose the analysis of eight different functions that are potential candidates to be used as error metric in the Calibration Stage of a forest fire spread forecast system. To study their strengths and lacks, we carried out a preliminary study to *artificially* compute the error of each function depending on its *Hits*, *False Alarms* and *Misses*. For this purpose, we consider a sample map with a number of real burnt cells equal to 55 ($RealCell = 55$). A simple and intuitive, way to test the behavior of a given error function consists of evaluating its value for all configurations of *Hits*, *Misses* and *False Alarms* when their values varies within the range [0 to 55]. With the computed errors we build a color map representation where the behavior of the Error function with regard to the *False Alarms* and the *Misses* is shown. On the right side of the color map, the legend will show a color scale for the error function values where blue color represents lowest errors, while red colour represents highest errors. In this section, we will use the described color map to understand the behaviour of all described error functions.

Our goal is to find an error function that grows faster as *Misses* increases rather than doing so as *False Alarms* increase, that is, solid error function candidates should present a *faster* variation along the *Misses* axis than along the *False Alarms* axis.

To facilitate the data processing, the elements of the contingency table are expressed in the context of difference between sets. The description of the conversion of these metrics is showed in the Table 1. Using this notation, in the subsequent sections, we shall describe different error functions that have been deployed in the above described Calibration Stage, and the advantages and drawbacks of each one are reported.

3.1 Bias Score or Frequency Bias (BIAS)

The *BIAS* score is the ratio of the number of correct forecasts to the number of correct observations [8]. Equation 1 describes this error function. This metric represents the normalized symmetric difference between the real map and the simulated map.

$$BIAS = \frac{Hits + FA}{Hits + Misses} \quad (1)$$

However, in the evolutionary process we focus on minimizing the ratio of the frequency of the erroneous simulated events, so we rely on a slight variation of the *BIAS* score. The same Error Function can be expressed in terms of the

Table 1. Elements of the contingency table expressed in the context of difference between sets.

RealCell	$Hits + Misses$	Cells burnt in real fire
SimCell	$Hits + FA$	Cells burnt in simulated fire
UCell	$Hits + Misses + FA$	Union of cells burnt in real fire and simulated one
ICell	$Hits$	Cells burnt in real fire and in simulated fire

difference between sets where the initial fire is considered a point and, therefore, it can be removed from the equation. The obtained formula is shown in Eq. 2.

$$\epsilon = \frac{Misses + FA}{Hits + Misses} = \frac{UCell - ICell}{RealCell} \tag{2}$$

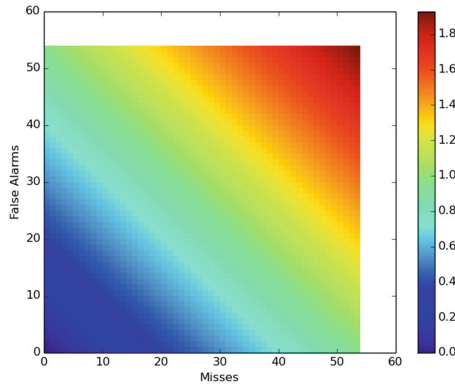


Fig. 2. Colour map representation of BIAS (Eq. 2).

In Fig. 2 the behaviour of the function 2 depending on *False Alarms* and *Misses* is shown. As it can be seen, the computed error grows up slightly faster in the *False Alarms* direction than in the *Misses* direction, this effect means that Eq. 2 lightly penalizes *False Alarms* compared to *Misses*.

3.2 BIAS+False Alarm Rate (BIAS+FAR) (ϵ_1)

This function is a combination of the previous formula (Eq. 2) and the *False Alarm Rate (FAR)*. The *FAR* measures the proportion of the wrong events forecast (see Eq. 3).

$$FAR = FA / (Hits + FA) \tag{3}$$

Since we are interested in penalizing those cases that underestimate the forecast, ϵ_1 combines BIAS and FAR. Equation 4 shows this new Fitness Function in terms of events and difference between cell sets.

$$\begin{aligned} \epsilon_1 &= \frac{1}{2} \cdot \left(\frac{Misses + FA}{Hits + Misses} + \frac{FA}{Hits + FA} \right) \\ &= \frac{1}{2} \cdot \left(\frac{UCell - ICell}{RealCell} + \frac{SimCell - ICell}{SimCell} \right) \end{aligned} \tag{4}$$

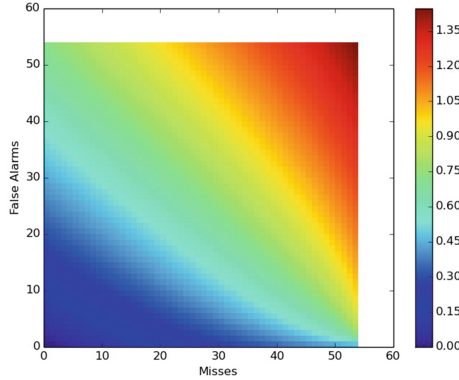


Fig. 3. Colour Map representation of BIAS+*FAR* (Eq. 4)

The behavior of this metric is shown in Fig. 3. As it can be seen, the variation of the error is not linear. The color map shows that while the blue part forms a convex curve, the yellow zone of the map forms a concave curve. It means that, while the amount of cells is low, the Eq. 4 penalizes more the *Misses* than the *False Alarms*, whereas with a large number of cells it tends to provide higher error for underestimated areas than for overestimated ones.

3.3 BIAS-False Alarm Rate (BIAS-*FAR*) (ϵ_2)

The next Error Function is quite similar to the previous equation (Eq. 4), but in this case the *FAR* is subtracted from the *BIAS*, as it is shown in the Eq. 5. As we said, *FAR* measures the rate of *False Alarms*, so the overestimated simulations have a high value of *FAR*. So, in this case, we subtract *FAR* from *BIAS* in order to provide a better position for those simulations that provide overestimated spread perimeters.

$$\begin{aligned} \epsilon_2 &= \frac{1}{2} \cdot \left(\frac{Misses+FA}{Hits+Misses} - \frac{FA}{Hits+FA} \right) \\ &= \frac{1}{2} \cdot \left(\frac{UCell-ICell}{RealCell} - \frac{SimCell-ICell}{SimCell} \right) \end{aligned} \tag{5}$$

The behavior of this metric is shown in Fig. 4. This figure shows that this metric presents a not linear behavior. We are able to see how the blue zone (low error) is bigger in the *False Alarms* axis than in the *Misses* one, it means that BIAS-FAR penalizes much more the *Misses* than the *False Alarms*. Moreover, a big green zone is present, where the computed error remains more or less constant. Above this green zone, we can see that the error grows faster in the *False Alarms* direction than in the *Misses* direction.

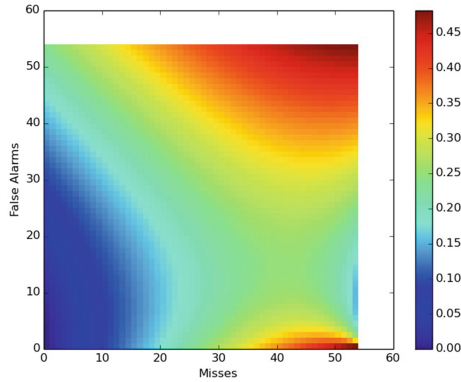


Fig. 4. Colour Map representation of BIAS-FAR (Eq. 5)

The main problem of this function is that for values around $Misses = 55$ and $FalseAlarms = 10$ (see Fig. 4), the error is lower than some simulations with better fitness. So, we cannot be confident about this metric, since it could cause that individuals with a better adjustment are discarded before individuals with a worse adjustment.

3.4 FAR+Probability of Detection of Hit Rate (FAR+POD) (ϵ_3)

The next Fitness Function used is a combination of Eq. 3 and the *Probability of Detection of hits rate (POD)*. The *POD* formula relates the observed events and estimated positively with all ones, Eq. 6. It represents the probability of a phenomenon being detected.

$$POD = \frac{Hits}{Hits + Misses} \quad (6)$$

However, as it was mentioned, we focus on minimizing the ratio of the frequency of the erroneous simulated events, so a slight variant of the *POD* is used, as expressed in formula 7.

$$\epsilon = \frac{Misses}{Hits + Misses} \quad (7)$$

The result of combining Eq. 7 with Eq. 3 is expressed in Eq. 8.

$$\begin{aligned} \epsilon_3 &= \frac{1}{2} \cdot \left(\frac{Misses}{Hits+Misses} + \frac{FA}{Hits+FA} \right) \\ &= \frac{1}{2} \cdot \left(\frac{RealCell-Icell}{RealCell} + \frac{SimCell-ICell}{SimCell} \right) \end{aligned} \tag{8}$$

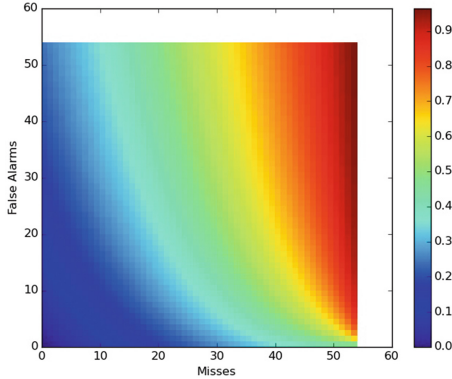


Fig. 5. Colour Map representation of FAR+POD (Eq. 8)

In Fig. 5, we can see that, while *False Alarms* are low, the error grows more slowly in the *Misses* direction than when the amount of *False Alarms* is high. In the same way, when the number of *Misses* is low, the error remains more or less constant in the *False Alarms* direction, but when the amount of *Misses* increases, the error grows up very fast in the *False Alarms* direction.

3.5 BIAS+Incorrectness Rate (BIAS+IR) (ϵ_4)

This Error Function was proposed in [3]. Using this function, the individuals that provide overestimated prediction have a better error than those individuals that underestimate the fire evolution. This function is shown in Eq. 9.

$$\begin{aligned} \epsilon_4 &= \frac{1}{2} \cdot \left(\frac{Misses+FA}{Hits+Misses} + \frac{Misses+FA}{Hits+FA} \right) \\ &= \frac{1}{2} \cdot \left(\frac{UCell-Icell}{RealCell} + \frac{UCell-ICell}{SimCell} \right) \end{aligned} \tag{9}$$

Figure 6 depicts the behaviour of this metric. As it can be seen, it shows a predominance of blue color, which means that the error grows very slowly. This might suggest that the errors obtained are very good in any case, but in the reality what happens is that this function practically treated every case, i.e., overestimated simulations and underestimated ones, in the same way. It is for a large number of cells where equation BIAS+IR provide lower errors for overestimated simulations than for underestimate simulations.

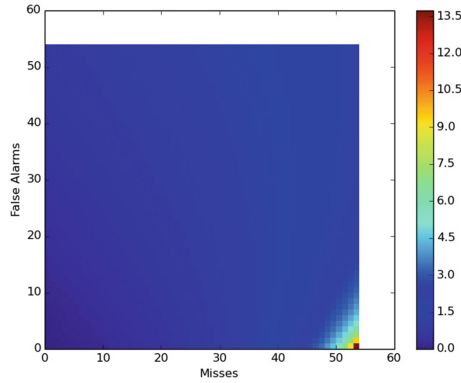


Fig. 6. Colour Map representation of BIAS+IR (Eq.9)

3.6 Adjustable Incorrectness Aggregation (AIA) (ϵ_5)

As we said, we look for an equation that penalize more the underestimated simulated areas than the overestimated, this implies that *Misses cells* are worse than *False Alarms cells*. In order to penalize more *Misses* than *False Alarms* the Eq. 10 was proposed

$$\epsilon_5 = \alpha \cdot FA + \beta \cdot Misses = \alpha \cdot (SimCell - ICell) + \beta \cdot (RealCell - ICell) \quad (10)$$

with $\alpha = 1$ and $\beta = 2$. This Fitness Function provides very high errors, but, in our case, this is not a problem, because we only want to compare the errors among the individuals but not the absolute value of the error.

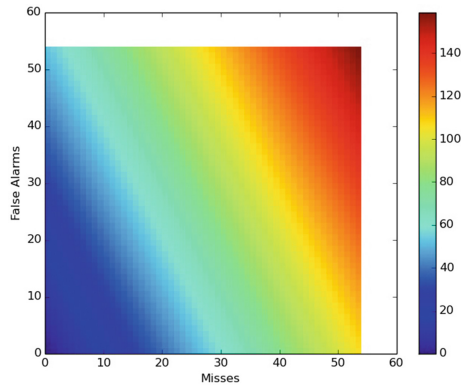


Fig. 7. Colour Map representation of AIA (Eq. 10)

Figure 7 represents the behaviour of this metric. As it can be observed, this metric clearly reproduces the behavior that we were expected. It is easy to see

that Eq. 10 penalizes more the *Misses* than the *False Alarms*, which is what we are looking for.

3.7 AIA with Correctness BIAS (AIA+CB) (ϵ_6)

This equation is close to Eq. 10 but, in this case, the *Hits* are removed (see Eq. 11). This implies that when using this error function, negatives values can be obtained but, as it was stated, we do not care about the value of the error but on the final ranking that is generated using it. In this case, the best individual will be the individual with a higher negative value.

$$\begin{aligned} \epsilon_6 &= \alpha \cdot FA + \beta \cdot Misses - \gamma \cdot Hits \\ &= \alpha \cdot (SimCell - ICell) + \beta \cdot (RealCell - ICell) - \gamma \cdot ICell \end{aligned} \tag{11}$$

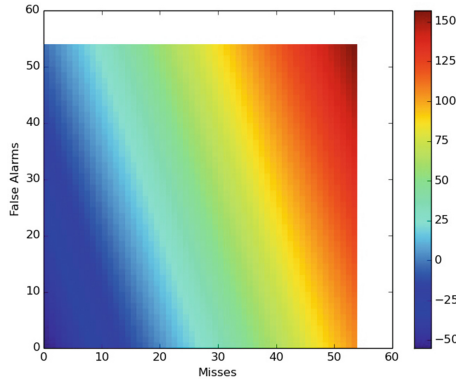


Fig. 8. Colour Map representation of AIA+CB (Eq. 11)

As in the previous case, using this metric, the error of the overestimated predictions increase slower than in the case of underestimated simulations (see Fig. 8). The problem of Eqs. 10 and 11 is that the values of α , β , and γ are fixed and they are not the best choice for all forest fires.

3.8 Ponderated FA-MISS Rate (PFA-MR) (ϵ_7)

In order to overcome the restrictions of Eqs. 10, 12 has been proposed.

$$\epsilon_7 = \alpha \cdot FA + \beta \cdot Misses \tag{12}$$

with

$$\alpha = \frac{Hits}{Hits + FA} = \frac{ICell}{SimCell} \tag{13}$$

and

$$\beta = \alpha + \frac{Hits}{Hits + Misses} = \frac{ICell}{SimCell} + \frac{ICell}{RealCell} \tag{14}$$

Then, the Error Function expressed in context of difference between sets corresponds to Eq. 15.

$$\epsilon_7 = \frac{ICell}{SimCell} \cdot (SimCell - ICell) + \left(\frac{ICell}{SimCell} + \frac{ICell}{RealCell} \right) \cdot (RealCell - ICell) \quad (15)$$

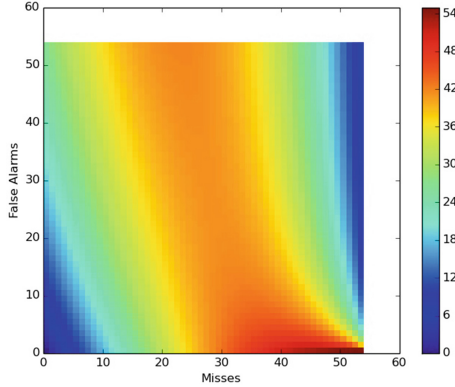


Fig. 9. Color Map representation of PFA-MR (Eq. 11)

In Fig. 9 the behavior of Eq. 15 is shown. As it was expected, it can be seen that this metric penalizes the *Misses* above the *False Alarms*. However, similarly to the case of *BIAS-FAR*, it behaves in a way that, in cases with high values of *Misses* (combined, in this case, with high values of *False Alarms*), it returns low error values. The big orange zone, between 20 and 45 *Misses* value, means that the maximum value of the error is achieved within this area. This implies that a large number of *Misses* can distort the selection of those individuals with a better fitting.

Based on the previous analyses and interpretations of the different proposed Error Functions, in the subsequent section we present an applied test using both synthetic and real results of a large fire that took place in Greece in 2011.

4 Experimental Study and Results

In order to analyze how the use of different error functions affects the prediction of the forest fire spread, we have selected as study case one event stored in the database of EFFIS (*European Forest Fire Information System*) [5]. In particular, we have retrieved the information of a past fire that took place in Greece during the summer season of 2011 in the region of Arkadia. The forest fire began on the

26th of August, and the total burnt area was 1.761 ha. In Fig. 10, it can be seen the fire perimeters at three different time instants: t_0 (August 26th at 09:43am) called *Perimeter 1*, t_1 (August 26th at 11:27am) corresponds to *Perimeter 2* and t_2 (August 27th at 08:49am) is *Perimeter 3*. The Two-Stage predictions strategy based on the Genetic Algorithm has been applied where the *Perimeter 1* was used as initial perimeter (ignition Perimeter), *Perimeter 2* was used in the Calibration Stage and the perimeter to be predicted is *Perimeter 3*.

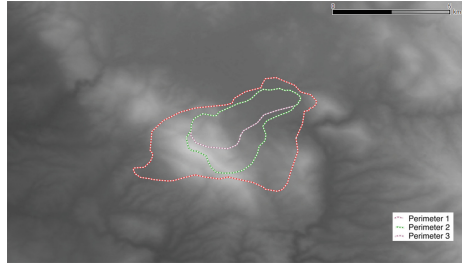


Fig. 10. Fire perimeters corresponding to the Arkadia fire.

Figure 11 shows the forest fire spread obtained using best individual at the end of the Calibration Stage and the forecast delivered using that individual for each error function defined in the previous section. As it can be observed, the fire evolution provided by the best individual at the end of the Calibration Stage is directly related to the Error Function applied. Using the POD+FAR and AIA+CB errors functions, the obtained best individuals fits well enough the bottom of the fire, see Fig. 11(d) and (g), but they overestimate the top very much. This could be a good result because it could happen that human intervention had stopped the real fire spread in that zone. However, the problem is that the corresponding predictions have a high overestimation of the burned area. The worst error formula is the seventh (PFA-MR), because the best individual obtained underestimates the real fire but the simulation in the Prediction stage has a very overestimate burned area.

In this case, the prediction that better fits the burned area is the simulation obtained when BIAS is used in the Calibration Stage (see 11(a)). This function provides the forecast with the highest number of intersection cells, although in some regions the burned area is overestimated. As we can see, the Error Function with the lower number of intersections cells are the AIA equation, Fig. 11(f). The predictions obtained from BIAS+FAR, BIAS-FAR and BIAS+IR, Fig. 11(b), (c) and (e) respectively, have less intersection cells than the prediction using BIAS but, at the same time, it has less *False Alarms*.

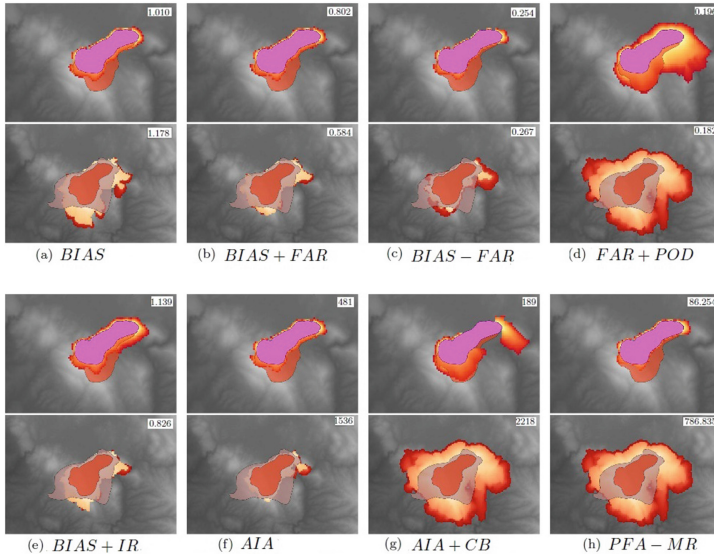


Fig. 11. For each error function (a) to (h), the upper figure shows the forest fire spread obtained using the best individual provided by the Calibration stage and the bottom figure depicts the final forecast delivered using that individual. The error evaluated for each case is also included

5 Conclusions

In the last years, the simulation of complex systems have demonstrated to be a powerful tool to improve the fight against natural hazards. For this reason, an adequate error function to evaluate the fitness of these models is a key issue. In this work, we focus on the specific case of wild fires as one of the most worrisome natural disaster.

In this work, eight equations have been tested in order to evaluate the prediction quality for large forest fires taking into account the factor of overestimated/underestimated predictions compared to the real fire. The results show that different error functions imply different calibration of the parameters and, therefore, different forest fire spread predictions are obtained. After applying the proposed error functions in the Two-Stage methodology, we can conclude that FAR+POD and AIA+CB functions tend to select individuals that provide very overestimated predictions. These functions provide the fittest individual in the Calibration Stage. The problem is, that using the adjusted inputs in these cases, the obtained predictions present very overestimated burnt areas. The function that underestimated more the fire perimeter is the sixth Error function (AIA), using this equation, the obtained prediction is the one with fewer intersection cells. The PFA-MR function is dismissed due to its lack of reliability.

There are a set of three Error Functions which stand out above others. These equations are BIAS, BIAS+FAR and BIAS+IR. As a result of our experimental

study, we can observe that we obtain more favorable results with this set of functions than with the rest. However, we are not able to determine undoubtedly which Equation is best for most of the cases. For this reason, our future work will be oriented to differentiate large fires of small fires, or fires with different meteorological conditions (wind prominence, mainly), in order to determine which Error function is more suitable, depending on these aspects.

Acknowledgments. This research has been supported by MINECO-Spain under contract TIN2014-53234-C2-1-R and by the Catalan government under grant 2014-SGR-576.

References

1. Abdalhaq, B., Cortés, A., Margalef, T., Luque, E.: Enhancing wildland fire prediction on cluster systems applying evolutionary optimization techniques. *Future Generation Comp. Syst.* **21**(1), 61–67 (2005). <https://doi.org/10.1016/j.future.2004.09.013>
2. Bennett, N.D., et al.: Characterising performance of environmental models. *Environ. Model. Software* **40**, 1–20 (2013)
3. Brun, C., Cortés, A., Margalef, T.: Coupled dynamic data-driven framework for forest fire spread prediction. In: Ravela, S., Sandu, A. (eds.) *DyDESS 2014*. LNCS, vol. 8964, pp. 54–67. Springer, Cham (2015). https://doi.org/10.1007/978-3-319-25138-7_6
4. Cencerrado, A., Cortés, A., Margalef, T.: Response time assessment in forest fire spread simulation: an integrated methodology for efficient exploitation of available prediction time. *Environ. Model. Software* **54**, 153–164 (2014). <https://doi.org/10.1016/j.envsoft.2014.01.008>
5. Joint Research Centre: European forest fire information system, August 2011. <http://forest.jrc.ec.europa.eu/effis/>
6. Ebert, B.: Forecast verification: issues, methods and FAQ, June 2012. <http://www.cawcr.gov.au/projects/verification>
7. Finney, M.A.: FARSITE: fire area simulator-model development and evaluation. FRResearch Paper RMRS-RP-4 Revised 236, Research Paper RMRS-RP-4 Revised (1998)
8. Gjertsen, U., Ødegaard, V.: The water phase of precipitation: a comparison between observed, estimated and predicted values, October 2005. <https://doi.org/10.1016/j.atmosres.2004.10.030>